New Hybrid Films Based on Cellulose and Hydroxygallium Phthalocyanine. Synergetic Effects in the Structure and Properties

Vicente Parra,[†,‡] Manuel Rei Vilar,*[,‡] Nicolas Battaglini,[‡] Ana M. Ferraria,[§]
Ana M. Botelho do Rego,[§] Sami Boufi,[||] María L. Rodríguez-Méndez,[⊥] Egils Fonavs,[#]
Inta Muzikante,[#] and Marcel Bouvet*[,†]

*Laboratoire de Chimie Inorganique et Matériaux Moléculaires-CNRS, Université Pierre et Marie
Curie−Paris 6, and ESPCI, Paris, France, ITODYS-CNRS, Université Paris Diderot−Paris 7, Paris,
France, Centro de Química-Física Molecular, IST, Lisbon, Portugal, Laboratoire Sciences des Matériaux
et Environnement, Faculté de Sciences de Sfax, Sfax, Tunisia, Deptartamento de Química Física y Química
Inorgánica, ETS Ingenieros Industriales, Universidad de Valladolid, Valladolid, Spain, and Institute of
Solid State Physics, University of Latvia, Riga, Latvia*

Hydroxygallium phthalocyanine (HOGaPc) and cellulose (from a trimethylsilyl derivative) have been used as native elements for the preparation of a novel family of hybrid films. By spin-coating, both components allow the building of films with different configurations on various substrates in a controlled way. The particularities of these hybrid films have been characterized by a range of techniques such as Fourier transform infrared spectroscopy (FTIRS) in attenuated total reflection using multiple internal reflections (ATR/MIR), absorption ultraviolet and visible spectroscopy (UV−vis), X-ray photoelectron spectroscopy (XPS), atomic force microscopy (AFM), and surface potential measurements using the Kelvin−Zisman vibrating capacitor probe (KP). This enabled determination of the influence of cellulose on the arrangement of HOGaPc and, consequently, control of the relation between the structure and the properties of the films. Finally, gas sensor tests were performed to check the potentialities of these hybrid films. In particular, the synergetic behavior between the film-forming materials allows a fast and sensible change in surface potential after cyclic exposures to ozone (O_3, 100 ppb) and nitrogen. Overall, we present the advantages of combining phthalocyanine with cellulose in enhancing the properties of the final product. Introduction of cellulose as a host material opens up a new area of hybrid films.

1. Introduction

Among functional materials owning electrical, optical, or mechanical properties, hybrid materials play an increasing important role in new technologies. Indeed, the synergetic combination of two or more compounds can enhance or produce new properties. For example, a hybrid system made from a polymer and a small molecule can combine the physical skills of the molecule, for example the optical ones, and the mechanical properties of the polymer used as a support. In addition, the polymer can improve the processability of the guest material. Therefore, new devices have been recently developed using hybrid materials.[1] In the case of polymer-based materials, the literature collects a large number of hybrid films having applications in recent topics such as electroluminescent devices,[2] sensors,[3] or photovoltaic cells.[4] In addition, it should be highlighted that the bindings between polymers (host) and functional materials (guest) can be carried out not only via weak interactions but also thanks to covalent bonds.[5]

Regarding the use of molecular materials as functional elements for hybrid films formation, the metallophthalocyanines (MPcs) really constitute a figure-of-merit. This is due to the large interest and physicochemical skills of MPcs as active materials in organic electronics applications.[6−9] Actually, they offer three important advantages: (i) high thermal and chemical stability compared with most of molecular materials; (ii) a rich substitution chemistry, leading to a vast amount of compounds with modulated properties; (iii) a very good processability, leading to the accomplishment

* To whom correspondence may be addressed. M. Rei Vilar: 1, Rue Guy de la Brosse, F-75005 Paris, France; tel, +33 1 44279978; fax, +33 1 44276814; e-mail, reivilar@paris7.jussieu.fr. M. Bouvet: 4, Place Jussieu, F-75005 Paris, France; tel, +33 1 44273083; fax, +33 1 44273841; e-mail, marcel.bouvet@espci.fr.

† Laboratoire de Chimie Inorganique et Matériaux Moléculaires-CNRS, Université Pierre et Marie Curie−Paris 6, and ESPCI.

‡ ITODYS-CNRS, Université Paris Diderot−Paris 6.

§ Centro de Química-Física Molecular, IST, Lisbon, Portugal.

|| Laboratoire Sciences des Matériaux et Environnement, Faculté de Sciences de Sfax, Tunisia.

⊥ Deptartamento Química Física y Química Inorgánica, ETS Ingenieros Industriales, Universidad de Valladolid.

Institute of Solid State Physics, University of Latvia.

(1) (a) Gómez-Romero, P. *Adv. Mater.* **2001**, *13*, 163. (b) Gómez-Romero, P.; Sánchez, C. *New. J. Chem.* **2005**, *29*, 57. (c) Cuentas-Gallegos, A. K.; Lira-Cantú, M.; Casan-Pastor, N.; Gómez-Romero, P. *Adv. Funct. Mater.* **2006**, *15*, 1125. (d) Baibarac, M.; Gómez-Romero, P. *J. Nanosci. Nanotechnol.* **2006**, *6*, 289. (e) McEvoy, T. M.; Long, J. W.; Smith, T. J.; Stevenson, K. J. *Langmuir* **2006**, *22*, 4462.

(2) Castelvetro, V.; De Vita, C. *Adv. Colloid Interface Sci.* **2004**, *108*, 167.

(3) Okada, A.; Usuki, A. *Mater. Sci. Eng., C* **1995**, *3*, 109.

(4) Walcarius, A. *Chem. Mater.* **2003**, *13*, 3351.

(5) Cannizo, C.; Mayer, C. R.; Secheresse, F.; Larpent, C. *Adv. Mater.* **2005**, *17*, 2888.

(6) (a) Bouvet, M. *Anal. Bioanal. Chem.* **2006**, *384*, 366. (b) Su, W.; Jiang, J. Z.; Xiao, K.; Chen, Y. L.; Zhao, Q. Q.; Yu, G.; Liu, Y. Q. *Langmuir* **2005**, *21*, 6527.

(7) (a) Wohrle, D.; Kreienhoop, L.; Schnurpfeil, G.; Elbe, J.; Tennigkeit, B.; Hiller, S.; Schlettwein, D. *J. Mater. Chem.* **1995**, *5*, 1819. (b) Salzman, R. F.; Xue, J. G.; Rand, B. P.; Alexander, A.; Thompson, M. E.; Forrest, S. R. *Org. Electron.* **2006**, *6*, 242. (c) Peumans, P.; Yakimov, A.; Forrest, S. R. *J. Appl. Phys.* **2003**, *93*, 3693. (d) Amao, Y.; Komori, T. *Langmuir* **2003**, *19*, 8872.

(8) (a) Cui, J.; Huang, Q. L.; Veinot, J. C. G.; Yan, H.; Wang, Q. W.; Hutchison, G. R.; Richter, A. G.; Evmenenko, G.; Dutta, P.; Marks, T. J. *Langmuir* **2002**, *18*, 9958. (b) Cheng, C. H.; Fan, Z. Q.; Yu, S. K.; Jiang, W. H.; Wang, X.; Du, G. T.; Chang, Y. C.; Ma, C. Y. *Appl. Phys. Lett.* **2006**, *88*, 213505.

(9) (a) Bouvet, M.; Pauly, A. In *The Encyclopedia of Sensors*; Grimes, C. A., Dickey, E. C., Pishko, M. V., Eds.; American Scientific Publishers: Stevenson Ranch, CA, 2006; Vol. 6, p 227. (b) Parra, V.; Hernando, T.; Rodríguez-Méndez, M. L.; De Saja, J. A. *Electrochim. Acta* **2004**, *49*, 5177. (c) Rella, R.; Serra, A.; Siciliano, P.; Tepore, A.; Valli, L.; Zocco, A. *Langmuir* **1997**, *13*, 6562. (d) Wang, H. Y.; Lando, J. B. *Langmuir* **1994**, *10*, 790.

of a large variety of solid phases by several deposition methods. Therefore, it is possible to build solid devices.

Concerning the host material, we have chosen the cellulose, the most abundant polymer on the earth. It is a carbohydrate polymer made from repeating β-D-glucopyranose moieties that are covalently bound through acetal functions between the equatorial OH group of C4 and the C1 carbon atom (β-1,4-glucan). The potentialities of this polymer are currently being explored through interdisciplinary research into its properties of hydrophilicity, chirality, biodegradability, biocompatibility, and reactivity, enabling large chemical modifying ability. Furthermore, potential formation of versatile semicrystalline fiber morphologies should also be mentioned.[10] Regarding the formation of hybrid films, cellulose is a material whose structure offers a profitable chance of modification by physical or chemical adsorption of molecules, leading to a wide range of hybrid systems. As examples, this polymer has been applied as a supporting material for nanoparticles,[11] as a template for nanofabrication of oxide structures,[12] in molecular recognition,[13] and in sensors based on a variety of transduction principles. In this regard, the literature includes cellulose-based films in humidity sensors,[14] modified cellulose surfaces with porphyrins in cyanide sensors,[15] optical detection of amino acids,[16] nitrite sensing,[17] etc. These examples point out the great versatility and advantages of cellulose when one thinks about supporting materials for hybrid films preparation. As cellulose is not a common organic solvent (or water)-soluble polymer, it is usually handled in a derivatized form. One of the most applied chemical modifications of cellulose is its silylation.[18] This allows the formation of cellulose films from solutions of silylated derivatives (CELL-Si). After a simple regeneration process consisting of a vapor phase acid hydrolysis from hydrochloric solutions,[19] the regenerated film is obtained (CELL-R).

In this work, we introduce cellulose as a useful supporting material in hybrid thin film formation, taking hydroxygallium phthalocyanine (HOGaPc) as a model functional material (Chart 1), in order to check the influence exerted by cellulose on its properties. So, to determine particular behaviors regarding synergetic effects in the films, we present a complete characterization of these novel hybrid films. As potential application, we aimed to the development of gas-sensing elements in sensor devices. An advantageous feature of these novel films is its easiness of processing. The choice of HOGaPc was due to three basic reasons: (i) its special solubility, which allows spin-coating to be used by successive deposition of solution aliquots without loss of material; (ii) the fact that its −OH group is axially linked to the metal offers a certain structural compatibility with the chemical structure of cellulose due to its hydroxyl content; (iii)

Chart 1. Chemical Structures of the Film-Forming Materials
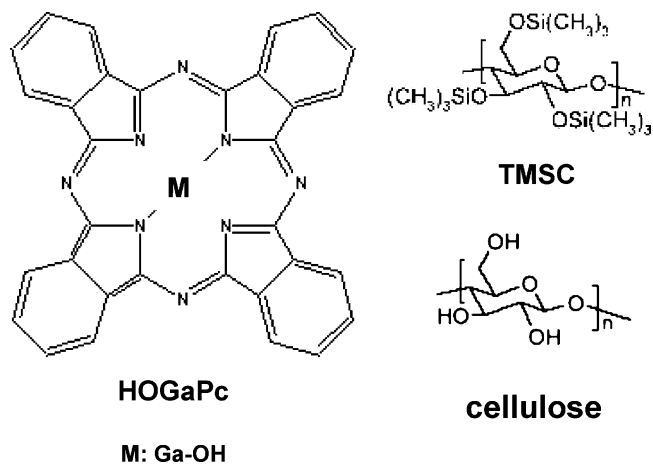
HOGaPc is a nonplanar phthalocyanine that possesses interesting photoelectronic properties explored on applications as sensor imaging[20] and optical limiting.[21] Furthermore, the HOGaPc properties, like those of other polymorphic phthalocyanines such as titanyl (TiOPc) or vanadyl (VOPc) derivatives, are strongly related to its crystalline structure in thin films,[22,23] and they present well-defined electron absorption patterns depending on the polymorphic structure. Thus, we can profit from UV−vis spectroscopy as a simple and useful tool to gain information about its structure in the film surroundings.

We will consider also some potential applications of these novel films, in the topic of gas sensors. Their performances as a gas-sensing element involve complex physicochemical mechanisms that are the basis of its detection limit, selectivity, repeatability, and reproducibility. Thus, major knowledge of the properties of the films, namely, molecular organization, morphology, and structure, becomes critical to support the above-mentioned chemical sensor features. Therefore, in this study, different types of films (covering both indium tin oxide (ITO) and undoped GaAs substrates) based on both constituents were characterized in depth by means of techniques such as Fourier transform infrared spectroscopy (FTIRS) in attenuated total reflection using multiple internal reflections (ATR/MIR), absorption ultraviolet and visible spectroscopy (UV−vis), X-ray photoelectron spectroscopy (XPS), atomic force microscopy (AFM), and surface potential measurements using the Kelvin−Zisman vibrating capacitor probe (KP) method.

Finally, the surface potential changes measured by the KP after exposing films of different nature to active and nonactive gases in ambient atmosphere, namely, nitrogen and ozone (100 ppb), have allowed us to check the effect of cellulose in enhancing the sensing properties of the films. These experiments are framed into the molecular controlled semiconductor resistor (MOCSER) devices. These novel molecular-material-based devices deal with the changes in the electrostatic potential of films as the principle of transduction in gas sensing.[24,25]

(10) Klemm, D.; Heublein, B.; Fink, H. P.; Bohn, A. *Angew. Chem., Int. Ed.* **2005**, *44*, 3358.

(11) (a) Ruan, D.; Huang, Q.; Zhang, L. *Macromol. Mater. Eng.* **2005**, *290*, 1017. (b) Tans, S. J.; Miedema, R.; Geerligs, L. J.; Dekker, C. *Synth. Met.* **1997**, *84*, 733.

(12) Huang, J.; Matsunaga, N.; Shimanoe, K.; Yamazoe, N.; Kunitake, T. *Chem. Mater.* **2005**, *17*, 3513.

(13) (a) Huang, J.; Ichinose, I.; Kunitake, T. *Angew. Chem., Int. Ed.* **2006**, *45*, 2883. (b) Blackburn, R. S.; Harvey, A.; Kettle, L. L.; Payne, J. D.; Russell, S. J. *Langmuir* **2006**, *22*, 5636−5644.

(14) Kusano, H.; Kimura, S.−I.; Kitagawa, M.; Kobayashi, H. *Thin Solid Films* **1997**, *295*, 53.

(15) Legako, J. A.; White, B. J.; Harmon, H. J. *Sens. Actuators, B* **2003**, *91*, 128.

(16) Awawdeh, M. A.; Legako, J. A.; Harmon, H. J. *Sens. Actuators, B* **2003**, *91*, 227.

(17) Ensafi, A. A.; Kazemzadeh, A. *Microchem. J.* **2002**, *72*, 193.

(18) McCormick, C. L.; Callais, P. A.; Hutchinson, H. L., Jr. *Macromolecules* **1985**, *18*, 2394.

(19) (a) Buchholz, V.; Adler, P.; Bäcker, M.; Hölle, W.; Simon, A.; Wegner, G. *Langmuir* **1997**, *13*, 3206. (b) Kontturi, E.; Thüne, P. C.; Niemantsverdriet, J. W. *Langmuir* **2003**, *19*, 5735.

(20) Street, R. A.; Graham, J.; Popovic, Z. D.; Hor, A.; Ready, S.; Ho, J. *J. Non-Cryst. Solids* **2002**, *299−302*, 1240.

(21) Chen, Y.; Hanack, M.; Arakic, Y.; Ito, O. *Chem. Soc. Rev.* **2005**, *34*, 517.

(22) Del Caño, T.; Parra, V.; Rodríguez-Méndez, M. L.; Aroca, R. F.; De Saja, J. A. *Appl. Surf. Sci.* **2005**, *246*, 327.

(23) Yamasaki, K.; Okada, O.; Inami, K.; Oka, K.; Kotani, M.; Yamada, H. *J. Phys. Chem. B* **1997**, *101*, 13.

(24) Cahen, D.; Naaman, R.; Vager, Z. *Adv. Funct. Mater.* **2005**, *15*, 1571.

(25) Rei Vilar, M.; El-Beghdadi, J.; Debontridder, F.; Naaman, R.; Arbel, A.; Ferraria, A. M.; Botelho Do Rego, A. M. *Mat. Sci. Eng., C* **2006**, *26*, 253.
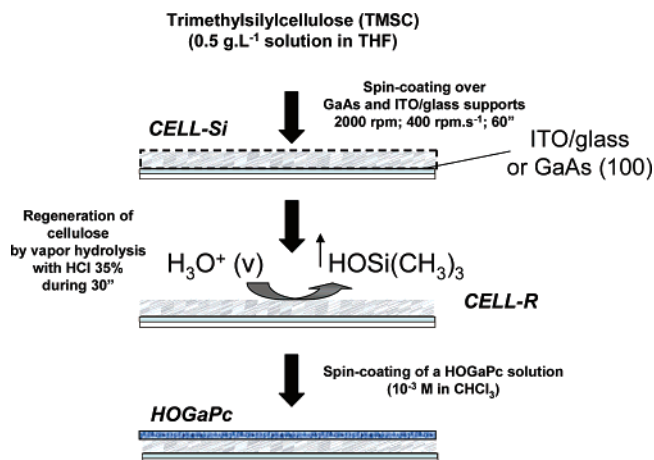
Figure 1. Scheme of the procedure of the hybrid film preparation. (1) Spin-coating of TMSC solution over GaAs or ITO/glass. (2) Vapor hydrolysis to form a regenerated or pure cellulose film. (3) Spin-coating of a HOGaPc solution.

2. Experimental Section

2.1. Materials and Chemicals. As cellulose is not a common soluble polymer, the original cellulosic material was trimethylsilylcellulose (TMSC), which was prepared from pure bleached cellulose fibers following previously reported methods[18] and dissolved in a mixture of toluene/tetrahydrofuran (THF) (50/50 vol %) at 0.5 g·L^{-1}. Hydroxygallium phthalocyanine (HOGaPc) was synthesized according to Yamasaki et al.[23] This compound was fairly soluble in a number of solvents, such as ethanol, THF, chloroform (CHCl$_3$), and toluene, in a range from 10^{-5} to 10^{-3} mol·L^{-1}. CHCl$_3$ was chosen as solvent. All reagents and solvents were Analytical Grade and used as supplied. Substrates were (i) undoped semi-insulating single-crystal GaAs wafers with orientation (100) acquired from American Crystals Technology (AXT) and (ii) ITO layers 100 nm thick sputtered on glass (40−50 Ω sheet resistance) acquired from Laboret Solems.

2.2. Sample Preparation. The used protocol for film preparation is illustrated in Figure 1. The film-forming materials were deposited by spin-coating at 2000 rpm, during 60 s, applying an acceleration of 400 rpm s^{-1}, over GaAs and ITO/glass substrates. CELL-Si films are obtained by spin-coating TMSC on the substrate, which after regeneration can be converted to cellulose films (CELL-R). On the other hand, three types of films containing HOGaPc were prepared: (i) pure HOGaPc films, formed by different numbers of depositions (*x*-HOGaPc, *x* being the number of spin-coated layers); (ii) mixed hybrid films (CELL + HOGaPc), from a mixture 50% (v/v) of both solutions directly spun over the substrates and submitted to the same HCl vapors during some 30 s; (iii) overlying samples formed on CELL-R by depositing a different number of spin-coated aliquots (*x*-HOGaPc/CELL-R).

2.3. Characterization Techniques. 2.3.1. FTIRS in ATR/MIR Mode. Major faces of the ATR/MIR crystals, highly transparent to infrared radiation in the spectral range 650−4000 cm^{-1}, 800 ± 40 μm thick, were cut from GaAs (100) wafers in 40 mm × 15 mm rectangles and were optically polished to 45° beveled edges in an isosceles trapezoidal configuration. This enables the transmitted infrared beam to be subjected to about 25 total internal reflections on each side of the crystal. Infrared spectra were recorded using a Magna-IR Nicolet 850 equipped with a MCT detector. Spectral resolution was 4 cm^{-1}.

2.3.2. UV−vis Spectroscopy. The electronic absorption spectra of CHCl$_3$ solutions (UV−vis spectrum in Supporting Information, Figure S1) and spin-coated films covering ITO/glass supports were recorded with a double beam UV−visible Shimadzu 2101 spectrometer in the range 900−280 nm.

2.3.3. X-ray Photoelectron Spectroscopy (XPS). The XPS spectrometer used was a XSAM800 (KRATOS) operated in the fixed analyzer transmission (FAT) mode, with a pass energy of 20

eV and the nonmonochromatised Mg Kα and Al Kα X-radiation (*hν* = 1253.7 and 1486.7 eV, respectively). The power was set to 120 W. Samples were analyzed in an ultra-high-vacuum (UHV) chamber (∼10^{-7} Pa) at room temperature, using take-off angles (TOA) of 90° and 30° as measured from the surface. Spectra were recorded by a Sun SPARC Station 4 with Vision software (KRATOS) using a step of 0.1 eV. A Shirley background was subtracted, and curve fitting for component peaks was carried out using Gaussian−Lorentzian products. X-ray source satellites were subtracted. No charge compensation (flood-gun) was used. Binding energies were corrected by using as reference In 3d$_{5/2}$ binding energy in ITO equal to 444.6 eV. This binding energy was obtained from the XPS analysis of ITO substrate, where the binding energy was corrected relatively to the energy of aliphatic carbon at 285 eV. For quantification purposes, sensitivity factors were 4.74 for Ga 2p$_{3/2}$, 0.42 for N 1s, 0.66 for O 1s, 0.25 for C 1s, 6.5 for In 3d$_{5/2}$, and 7.2 for Sn 3d$_{5/2}$.

2.3.4. Atomic Force Microscopy (AFM). Tapping mode AFM (TM-AFM) images were recorded by commercial AFM equipment, Multimode Nanoscope III, at room conditions.

2.3.5. Surface Potential Measurements. The changes in the molecular dipole of film-forming molecules modify the surface potential (ΔU_s) of the thin films. These changes were measured using a Kelvin−Zisman vibrating capacitor probe (KP) with 1 mV resolution.[26] The KP is a noninvasive technique used to measure ΔU_s between a vibrating Au plate (175 Hz) and a conducting (or partially conducting) nonmetallic specimen without touching the surface. All measurements were made at room temperature. A drop of silver paste served as electrical contact at a region of the film-free ITO. The surface potential of the films was measured as the difference between the value of the ITO electrode and that obtained when scanning the deposited films. The linear length of surface scanning was 17 mm.

2.3.6. Gas-Sensing Tests. The same KP was used as transduction technique of the surface dipole changes detected by the films after being submitted to different gas atmospheres (N$_2$ and O$_3$). All experiments were performed in air at room temperature. As cleaning gas, pure N$_2$ was used, whereas O$_3$ was applied as active gas. It was created with a portable ozone generator that supplied 100 ppb diluted in air.

3. Results and Discussion

3.1. FTIRS (ATR/MIR) Structure Analysis. FTIRS analysis in attenuated total reflectance and multiple internal reflections (ATR/MIR) was applied with the aim to record the spectra of films following three main criteria: (i) to monitor the chemical transformation of CELL-Si to CELL-R films; (ii) to monitor the multideposition process of HOGaPc; (iii) to check the compatibility of CELL-R with HOGaPc as well as the nature of the adsorption process. The penetration depth of the evanescent wave, being of the order of 1 μm,[27] allows the analysis of the whole thickness of the layer.

Figure 2a shows the ATR/MIR spectra (1550−650 cm^{-1}) of spin-coated films of CELL-Si and CELL-R. Important changes in both spectra are observed, in particular relative to the trimethylsilyl bands. Assignments of the different bands are given in Table 1.[28] These are the (Si−C) rocking vibrations appearing at 750 and 841 cm^{-1}, the (Si−O) stretching vibration at 1041 cm^{-1}, and finally the (−CH$_3$) symmetric deformation mode centered at 1250 cm^{-1}. All these bands, which entail a sort of signature of CELL-Si drastically decreased after subjecting the film to HCl vapors for 30 s. In addition, novel IR bands emerge, which are assigned to a typical cellulose film. Concerning the range 3800−2500 cm^{-1}, two principal modifications are observed

(26) Vitilis, O.; Fonavs, E.; Muzikante, I. *Latv. J. Phys. Tech. Sci.* **2001**, *5*, 38.

(27) Botelho Do Rego, A. M.; Ferraria, A. M.; El Beghdadi, J.; Debontridder, F.; Brogueira, P.; Naaman, R.; Rei Vilar, M. *Langmuir* **2005**, *21*, 8765.

(28) Socrates, G. *Infrared Characteristic Group Frequencies*, 2nd ed.; Wiley International Publication; John Wiley & Sons: Chichester, 1994.
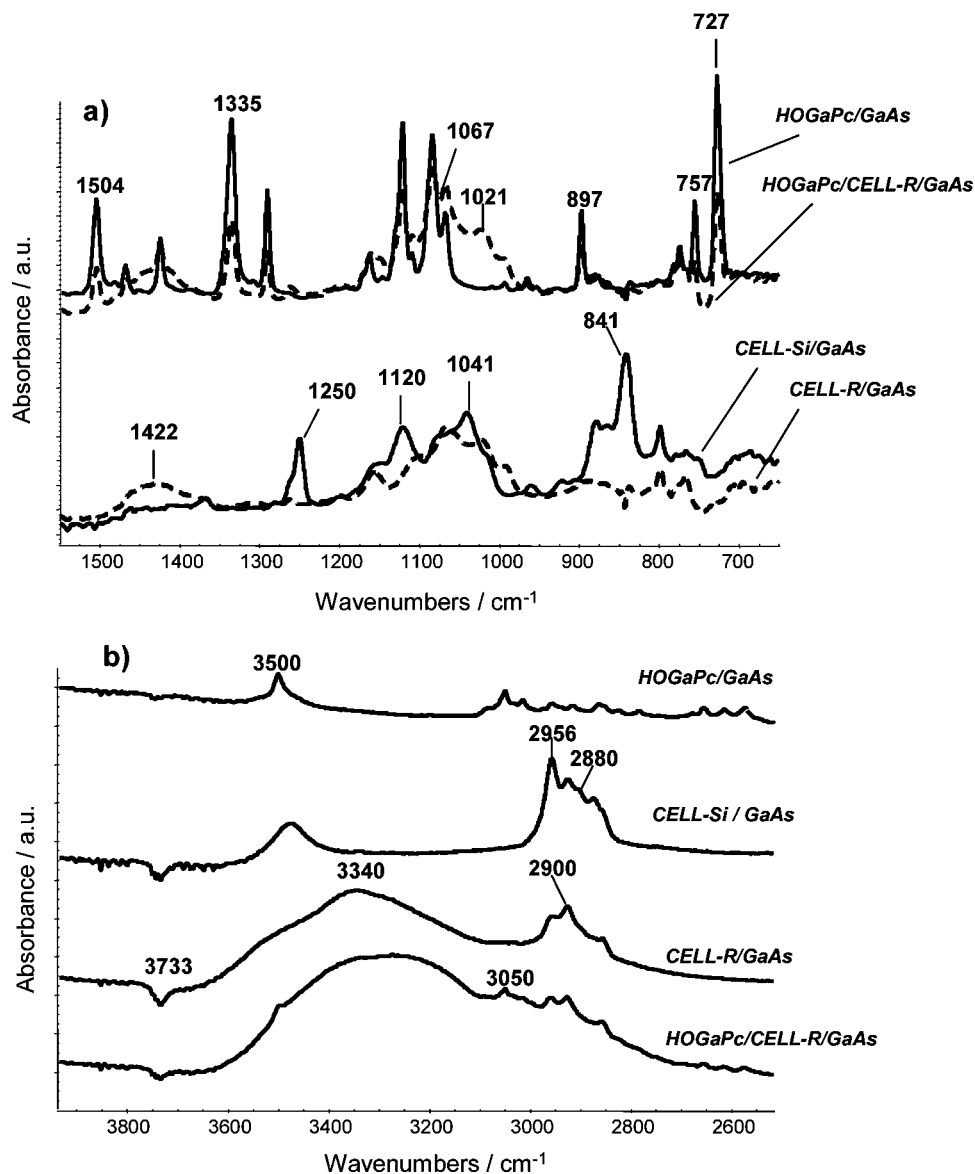
Figure 2. FTIRS in ATR/MIR mode spectra showing the most important features of some representative examples of both pure and hybrid films: (a) comparison between 1-HOGaPc/CELL-R/GaAs and 1-HOGaPc/GaAs (upper part) and CELL-R/GaAs and CELL-Si/GaAs (lower part) in the wavenumber region $1550-650$ cm^{-1}; (b) comparison between the four types of films in the region $3850-2550$ cm^{-1}.

when passing from CELL-Si to CELL-R films. Figure 2b illustrates the drastic decreasing evolution of the (CH$_3$) symmetric and asymmetric stretching bands at 2880 and 2956 cm^{-1}, respectively, which are due to the presence of the methylsilylated groups. However, we detect some residual methyl groups (CH$_3$ asymmetric stretching band) due to the non-100% yield of the O$-$Si bonds hydrolysis.

In addition, in the (OH) IR stretching region, at higher wavenumbers than 3100 cm^{-1}, there are also noticeable outcomes to discuss. CELL-Si film shows a fairly wide band that peaks at 3495 cm^{-1} that can be associated either to an incomplete $-$OH substitution in TMSC[18a] or to the adsorption of some amount of ambient water. On the contrary, in CELL-R film, we observe the appearance of a broad band from 2800 to 3700 cm^{-1}, with a maximum at ca. 3340 cm^{-1} indicating the presence of adsorbed water or mainly OH groups forming hydrogen bonds and testifying to the increase in hydrophilicity of the surface. In relation to the HOGaPc/CELL-R/GaAs film, the (aryl C$-$H) stretches at 3050 cm^{-1}, which keeps the same energy and shape as the HOGaPc/GaAs film and the (OH) mode of the phthalocyanine derivative (at ca. 3500 cm^{-1}). From these outcomes, we conclude that

HOGaPc is essentially physisorbed on the cellulose support. Nonetheless, the contour of the above stated large (OH) band changes moderately, becoming almost shapeless and even wider. Both the appearance and the change in shape of this band should be ascribed to the formation of the typical hydroxyl groups in cellulose and to the modification of the hydrogen-bonding interactions. The intensity of this representative band is also related to the effect of the room humidity.

Regarding the chemical compatibility of both film-forming materials, the ATR/MIR spectra of hybrid films can be considered as the sum of each component, as a result of the lack of IR band shifts. Thus, the process governing the interaction between cellulose and HOGaPc is essentially believed to be physisorption.

Additionally, ATR/MIR spectroscopy was applied to check the trend followed by HOGaPc after consecutive spin-coating over CELL-R. Figure 3 shows the spectra of a series of eight single layers spun successively, on the top of its preceding layer. The wavenumber range contains the most significant IR active bands for HOGaPc and CELL-R. At first glance, the spectra point out that HOGaPc can be deposited in a reproducible way, as evidenced by the comparable intensity and width of the peaks

Table 1. FTIRS Band Assignments for Both Film-Forming Materials in Spin-Coated Films (ATR/MIR) and in Other Forms Taken as References

(a) HOGaPc

HOGaPc/GaAs[a]	HOGaPc/KBr	assignments[b]
727	727	CH wagging oop
755	756	benzene (v_1)
774	772	C−H wagging
897	899	C−H bending ip
1067	1069	C−H bend ip
1084	1086	isoindole breathing or C−H bending (v_{18})
1121	1119	C−H bending ip
1162	1167	C−H bending (v_{9a})
1290	1288	benzene (v_{14})
1335	1337	C−N stretching (pyrrole)
1424	1425	isoindole stretching
1468	1470	benzene (v_{19b})
1504	1499	benzene (v_{19a})
1610	1612	benzene (v_{8a})
3050	3061	(benzene) C−H stretching
3500		O−H (Ga) stretching

(b) Cellulose-Based Materials

TMSC/GaAs[a]	cellulose/GaAs[a]	AVICEL[c]	assignments[b]
750			Si−C rocking
841			Si−C rocking
		895	γ(COC) ip symmetric stretching
	1021		
1041			Si−O stretching
	1067	1062	C−O−C asymmetric stretching
1120			Si−O stretching
	1152	1166	C−H and O−H deformation
1250			CH₃ deformation
	1422	1434	CH₂ symmetric bending
	1645	1642	associated O−H bending
2880			CH₃ symmetric stretching
	2900		CH₂ asymmetric stretching
2956			CH₃ asymmetric stretching
3494	3340	3380	associated O−H stretching
	3733		isolated OH stretching

[a] Spin-coated films. [b] Key: ip, in-plane; oop, out-of-plane. [c] Commercial product.
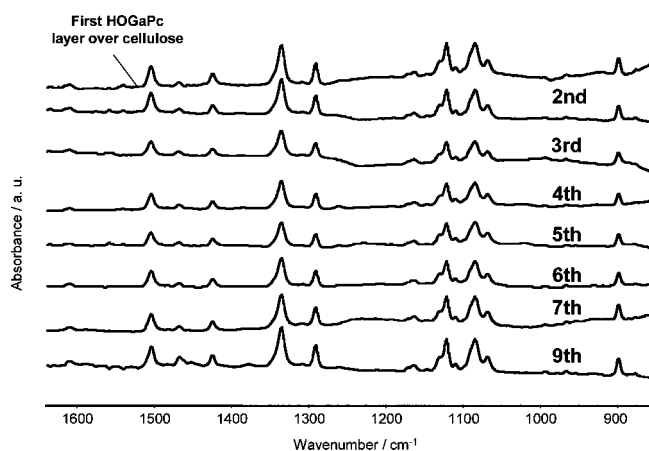

Figure 3. ATR/MIR spectra of multideposited amounts of HOGaPc by spin-coating on a CELL-R (the numbers indicate the number of deposition of HOGaPc). Each spectrum was recorded taking as the background the preceding one, so they represent individual HOGaPc spun films. All spectra are displayed in a common scale.

for several spin-coating processes. In addition, as each spectrum is recorded taking as background the previous one, the absence of negative bands is noticed. This fact indicates that no material is lost even after spin-coating new aliquots of the chloroform solution, revealing that the films are highly stable.

3.2. UV−vis Electronic Absorption Analysis. Changes in dipole−dipole interactions in phthalocyanine films can be observed by optical absorption spectroscopy, besides the optimization of the face-to-face interaction between π-cores. Therefore, we used UV−vis spectroscopy as a tool to study the structural changes of an excellent chromophore such as HOGaPc in different surroundings. The aim of this analysis was focused on the exerted structural effect of cellulose over HOGaPc. For this purpose, we used the well-defined UV−vis absorption patterns of the crystalline structures of nonplanar phthalocyanines,[22] as in the case of HOGaPc.[23]

If we compare all cellulose-based films with that of HOGaPc directly spun over the ITO support (1-HOGaPc/ITO) (Figure 4a), it is clearly observable how the band at ca. 830 nm is uniquely present in the case of the pure phthalocyanine film. Indeed, this band is ascribed to an excitonic intermolecular charge transfer (CT) that usually occurs when a face-to-face molecular arrangement is produced in the thin film, and it is sensitive to the film structure features.[22] Such an outcome suggests that cellulose tends to inhibit this molecular stacking, keeping the HOGaPc molecules in a rather amorphous state. The comparable spectra of CELL + HOGaPc and 1-HOGaPc/CELL-R films are worth mentioning, which implies that the first spin-coated film over CELL-R entails a phthalocyanine arrangement comparable to that of the mixed film; i.e., the phthalocyanine is randomly aggregated due to the cellulose effect.

With the aim to gain more information regarding the molecular film state of HOGaPc in pure and cellulose environments, Figure 4b shows an extended analysis. If one analyzes the relative intensities of the excitonic CT-band of both types of films, 1,2-HOGaPc/ITO and 2,3-HOGaPc/CELL-R/ITO, it is clear that the
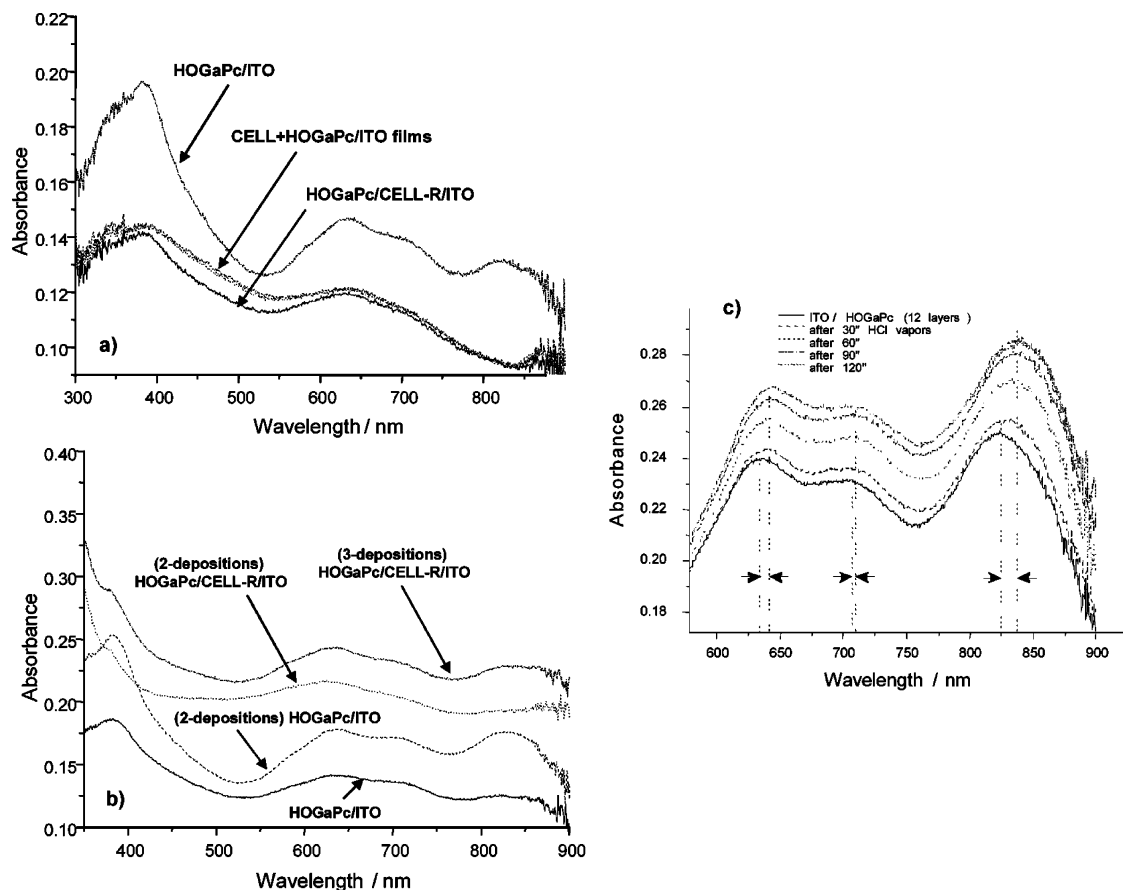
Figure 4. UV−vis electronic absorption spectra of different films based on cellulose and HOGaPc: (a) and (b) pure HOGaPc and different hybrid films over ITO/glass, for comparison purposes regarding the different nature of the absorption bands; (c) effect of an acid vapor exposure (from 35% HCl solution) during progressive times.

biopolymer exerts a decisive effect on the HOGaPc structure. At the beginning, in ultrathin films, due to the wide and split phthalocyanine Q-band (between 550 and 750 nm), we suggest that there is some extent of aggregation in face-to-face stacking, but in a rather discontinuous way. Therefore, the incipient CT-related band begins to appear but it is accomplished with lack of real stacking (i.e., molecular order). On the other hand, by adding consecutive HOGaPc spin-coated films, their interaction is improved, leading to the transition from random aggregates to crystalline structures, or at least organized face-to-face interactions. This is extracted, for instance, from the absorption spectra of 12-HOGaPc/CELL-R (Figure 4c), which agrees with the reported crystalline forms of HOGaPc in thin films.[23]

To illustrate the different nature of the HOGaPc absorption bands, we submitted the 12-HOGaPc/CELL-R film to the progressive action of HCl vapors from 30 to 120 s (i.e., a vapor annealing, at room temperature). As shown in Figure 4c, it is evident that this treatment does not induce equivalent changes in each of the UV−vis bands from 640 to 825 nm. In particular, the CT-related band experienced a noticeable red-shifted evolution (up to 15 nm) after different intervals of vapor exposure. In contrast, the band at 715 nm, usually ascribed to the absorption of monomers, remained almost unaltered. Concerning the band with a maximum at 640 nm, only a slight shift of ca. 4 nm to lower energies was detected. These results indicate that the nature of the CT-exciton, related to the potential formation of a separated charge state (between a pair of molecules), is more environmental dependent than the other ones, which are rather associated to local or intramolecular excited states.

UV−vis electronic absorption spectroscopy is also a functional tool to check the features of the growing process of a large variety of multilayer films of chromophores.[29] Thus, UV−vis spectra of consecutive spin-coating aliquots of the HOGaPc solution over CELL-R/ITO were registered. Figure 5 illustrates both the spectra (a) and the linear fitting when plotting the HOGaPc peaks absorbance vs the number of layers (b), from 2 to 12 spun layers. From both the spectra and the corresponding linear regressions, it is obvious that the films exhibit a uniform and controlled supramolecular architecture after consecutive depositions. The fact that the straight lines in Figure 5b have positive intercepts (instead of 0) suggests that the first HOGaPc spun film entails the transfer of a higher amount of material over CELL-R. Moreover, the different evolution of the absorption bands has to be highlighted. In particular, the intensity of the CT-related absorption increases faster than the others. Following the same criterion as before, this is explained in terms of the extended molecular stacking due to the growth of HOGaPc after each spun film. Indeed, this also correlates with the AFM analysis of the multilayer films (cf. section 3.4), in which crystalline-like islands grew with the consecutive deposition process.

3.3. X-ray Photoelectron Spectroscopy (XPS). XPS is a technique able to identify and quantify the elemental composition at the surface region with an analysis depth of the order of 3−10 nm.[30] XPS was applied to monitor the amount of material transferred after each deposition. Additionally, this implies

(29) (a) Lowman, G. M.; Nelson, S. L.; Graves, S. A.; Strouse, G. F.; Buratto, S. K. *Langmuir* **2004**, *20*, 2057. (b) Del Caño, T.; Parra, V.; Rodríguez-Méndez, M. L.; Aroca, R.; De Saja, J. A. *Org. Electron.* **2004**, *5*, 107. (c) Parra, V.; Del Caño, T.; Coco, S.; Rodríguez-Méndez, M. L.; De Saja, J. A. *Surf. Sci.* **2004**, *550*, 106. (d) Su, W.; Jiang, J.; Xiao, K.; Chen, Y.; Zhao, Q.; Yu, G.; Liu, Y. *Langmuir* **2005**, *21*, 6527.

(30) Briggs, D.; Seah, M. P. *Practical Surface Analysis by Auger and X-ray Photoelectron Spectroscopy*; John Wiley & Sons: New York, 1985.
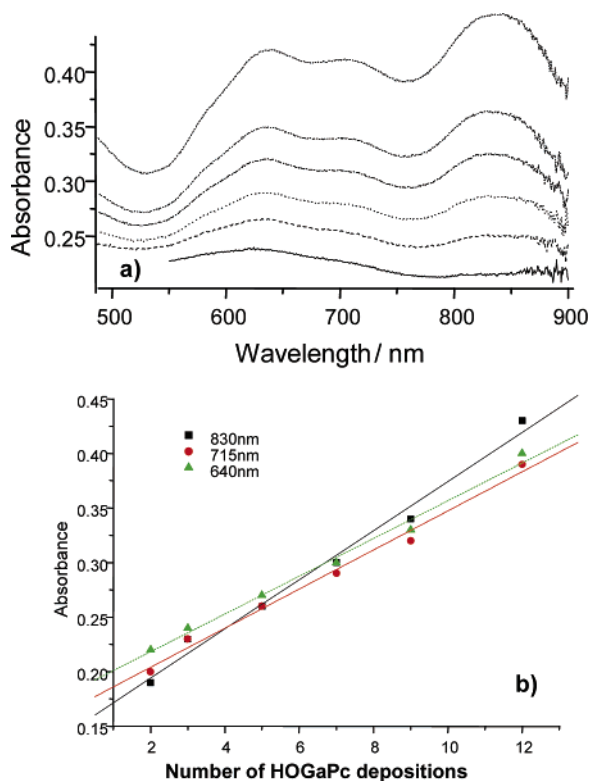
Figure 5. (a) UV−vis absorption spectra for spin-coated films on ITO/glass. From bottom to top, 2, 3, 5, 7, 9, and 12 depositions. (b) Absorbance of the three bands ca. 835 nm (■), 711 nm (●), and 635 nm (▲) vs number of depositions showing the linear fit trend followed by the bands. One can notice the particular behavior of the CT-related band at higher wavelengths.

knowledge about the trend followed by HOGaPc when it is growing with consecutive deposition by spin-coating. CELL-Si and CELL-R films have thicknesses estimated to be about 7−8 nm, which supposes the thinnest cellulose films attained up to now. Nevertheless, the substrate signal could be clearly seen and allowed the ratio C 1s/In 3d (from ITO) to be computed and used for the thickness estimation.

In particular, the relative amount of nitrogen and gallium existing in the HOGaPc-grafted film was quantified for samples prepared with a different number of HOGaPc depositions over CELL-R, namely, 1, 2, 3, 7, 9, and 12. N 1s and Ga 2p signals were taken as HOGaPc fingerprints and used to follow the evolution of the growing process. Figure 6 shows the N 1s/In 3d and Ga 2p/In 3d ratios resulting from the XPS analysis using Al Kα radiation. Results obtained with Mg Kα radiation follow the same trend. It is clear that the relative amounts of nitrogen and gallium increase for an increasing number of depositions of HOGaPc. Besides, this relative amount is greater for lower TOA, indicating a nonconstant concentration depth profile (photoelectrons detected at 30° are representative of a lower depth than those detected at 90°).[29] The experimental ratio N 1s/In 3d is, in fact, the (N 1s + Ga $L_2M_{45}M_{45}$)/In 3d ratio, since the N 1s region obtained with the Al X-ray source is overlapping the Auger structure Ga $L_2M_{45}M_{45}$ (Figure 6c). Moreover, the atomic ratios N 1s/In 3d and Ga 2p/In 3d are fitted by exponential functions of the type $y = a[1 − \exp(−bn)]$ compatible with a vertical growth of the island-like structures (n is the number of depositions and a and b are constants). However, the first three points could be fitted with a straight line, which is compatible with a horizontal growth of the film. Hence, we cannot discard the possibility of two different growth mechanisms.

Furthermore, the ITO XPS regions (In 3d and Sn 3d, for instance) are clearly detected and the ratio In 3d/Sn 3d is nearly constant, supporting that HOGaPc does not completely cover the substrate. As a consequence, the trend followed by the signals suggests that two types of growth take place between the earliest and final depositions: on the first deposition, we propose that HOGaPc only covers a fraction of the free CELL-R surface (X−Y plane of the substrate), but the subsequent depositions are rather occurring in a three-dimensional (3-D) way, all along the Z-axis. This kind of growth correlates well with that observed in tin phthalocyanine (SnPc) films prepared by MBE (molecular beam epitaxy).[31]

In addition, for a single deposition, interesting results are obtained when comparing the XPS spectra of 1-HOGaPc/ITO and 1-HOGaPc/CELL-R/ITO samples (Supporting Information, Figure S2). In fact, for 1-HOGaPc/ITO, weak Ga 2p signals having similar areas are obtained for TOA = 90 and 30°. The ratio Ga/In increases for TOA = 30° as expected, since the In signal is here more attenuated. However, for 1-HOGaPc/CELL-R/ITO, an astonishing difference between both analysis angles exists: For TOA = 90°, the Ga 2p signal is almost inexistent, rendering its area evaluation practically impossible. Nevertheless, for TOA = 30°, a measurable signal is obtained, having an area of the same order of magnitude as those obtained for the 1-HOGaPc/ITO case. This leads us to think that the gallium atoms are hidden in the cellulose cavities, being hardly detected. However, when the analysis angle varies, the cavity walls are perceived and the Ga atoms can deliver consequently a detectable signal. This behavior is not observable in the case of the nitrogen. In fact, nitrogen atoms always deliver XPS signals for both geometries, which can be explained since their photoelectrons are much more energetic than the Ga 2p ones (1086.5 vs 369.8 eV). The geometric effect observed for gallium atoms is then attenuated for nitrogen, where even for TOA = 90° their signal is still detected. Thickness and coverage fraction were estimated from the N/In values using both analysis angles. The evaluated thickness for the phthalocyanine film in 1-HOGaPc/ITO is then 2.4 ± 0.2 nm with a covered surface fraction of 0.75. For the 1-HOGaPc/CELL-R/ITO, assuming a thickness of 8 nm (a value suggested by the ratio C/In) for the cellulose film underneath the phthalocyanine film, a thickness of 0.5 nm and a coverage fraction of 0.95 were obtained. These results lead us to conclude that HOGaPc forms an island-like structure in the case of 1-HOGaPc/ITO, whereas when it is deposited over the cellulose film it is much more dispersed, with a higher coverage fraction. We can also conclude that the amount of phthalocyanine deposited on ITO is larger than that on cellulose (the product coverage fraction × thickness is larger in the first case). These last results are in good agreement with the UV−vis observations: (i) in the case of 1-HOGaPc/CELL-R/ITO, the lack of the band at ca. 830 nm, prominent in 1-HOGaPc/ITO, indicates a nonoptimized interaction between pairs of molecules because of the attenuation effect exerted by cellulose in the HOGaPc aggregation; (ii) the absorbance of HOGaPc/ITO, in comparison with that of HOGaPc/CELL-R/ITO, is higher.

3.4. Atomic Force Microscopy (AFM). AFM provided information about the aspect of the films and allowed us to correlate morphology and optical properties. In particular, taking into account the observed UV−vis spectroscopy features exhibited by the HOGaPc-based films, their involvement in arrangement in films is interesting.

(31) Vearey-Roberts, A. R.; Steiner, H. J.; Evans, S.; Cerrillo, I.; Mendez, J.; Cabailh, G.; O'Brien, S.; Wells, J. W.; McGovern, I. T.; Evans, D. A. *Appl. Surf. Sci.* **2004**, *234*, 131.
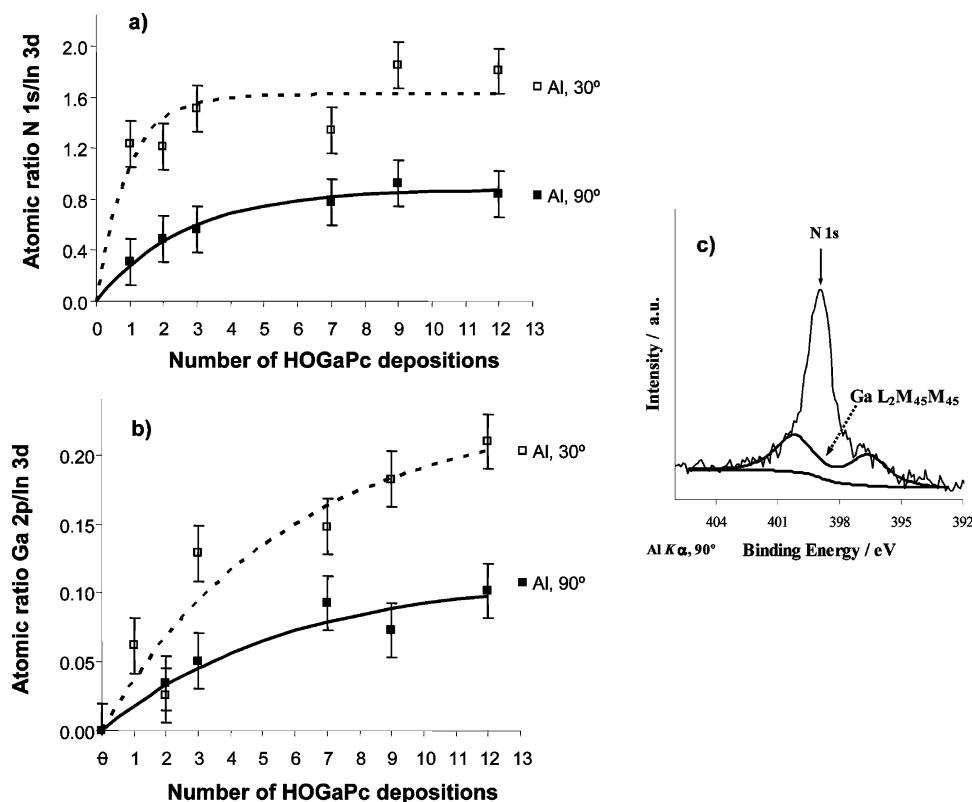
Figure 6. Relative amount of (a) nitrogen and (b) gallium existing in HOGaPc/CELL-R/ITO samples reported for In 3d. Data were obtained with the Al Kα source. Full and empty symbols represent atomic ratios acquired at TOA = 90° and 30°, respectively. Full and dashed lines are fitted curves to TOA = 90° and 30° points, respectively. Error bars: ±0.2 for N 1s/In 3d; ±0.02 for Ga 2p/In 3d. (c) Peak centered at ~399 eV containing N 1s photoelectron and Ga $L_2M_{45}M_{45}$ Auger.

Figure 7 shows a series of AFM images including the ITO/glass support, for comparison purposes, and some representative cellulose−HOGaPc films deposited over it.

ITO/glass film morphology (Figure 7a) consisted of a granular structure giving an R_q value of 1.3 nm typical of a particularly smooth surface.[32]

The AFM image of a CELL-R (Figure 7b) shows a homogeneous surface, with an R_q of 2.1 nm, indicating an especially smooth film covering all the ITO substrate. When the mixed solution is spun and subsequently hydrolyzed (CELL + HOGaPc), a film with a completely different morphology is formed (Figure 7c). One can observe a kind of linear structures connected all over the surface that entails a more porous surface than that seen in CELL-R. The brightest and darkest parts would be attributed to domains corresponding to the separation between the film-forming materials. This singular structure leads to an R_q of 1.8 nm, a value even lower than that of the pure CELL-R film.

Important differences can be visualized in the AFM image related to the 1-HOGaPc/CELL-R (Figure 7d). This bilayer-type deposition involves the formation of two markedly different structures. On one hand, there are regions where one can observe an extended cellulose-based support all along the scanned surface. On the other hand, one can distinguish the presence of protrusions attributed to HOGaPc islands (size ca. 200−220 nm) over the cellulose support. This morphology gives rise to an R_q value of 2.1 nm, equivalent to pure CELL-R.

In the case of multilayered HOGaPc films, interesting features are observed. Figure 7e illustrates the morphology of a 7-HOGaPc/ITO film. As one can clearly see, the phthalocyanine forms islands

(32) Betz, U.; Kharrazi Olsson, M.; Marthy, J.; Escolá, M. F.; Atamny, F. *Surf. Coat. Technol.* **2006**, *200*, 5751.

ca. 500 nm wide and 130 nm high, which are thought to come from the growth of the phthalocyanine nuclei mentioned above. This island-like morphology gives thus $R_q = 42$ nm and supports one fact: the more the amount of HOGaPc is spin-coated, the higher are the observed islands. This suggests that HOGaPc grows in a 3-D manner rather than covering the substrate.

On the other hand, if one analyzes the 7-HOGaPc/CELL-R/ITO film, we can observe an analogous trend. However, it was found that the growth of the islands is certainly influenced by the biopolymer, as Figure 7f illustrates. In this case, the HOGaPc islands are markedly lower in size and height (ca. 250 nm per 60 nm, respectively), resulting in a roughness $R_q = 26$ nm, and then a markedly smoother film than 7-HOGaPc/ITO.

From these outcomes, it should be noted that cellulose plays an important role in modulating the growing process of phthalocyanine structures. In other words, the polymer exerts an attenuating effect in the inherent aggregation tendency of HOGaPc during the multideposition process confirming UV−vis and XPS observations. Both spectroscopic analyses suggest the occurrence of a growing mechanism different from the first HOGaPc depositions. By UV−vis, we monitored the transition from amorphous-like to crystalline structures, due to the evolution of the electronic absorption patterns, in addition to a "diluting" effect of cellulose over HOGaPc aggregation, mainly in the first spun films; in XPS, two different trends were exhibited during the molecular growth, showing also evidence of a nontotal coverage of the cellulose support.

3.5. Gas-Sensing Tests by KP Measurements. The KP technique is a powerful tool that is able to measure changes in surface potential differences between a reference material and
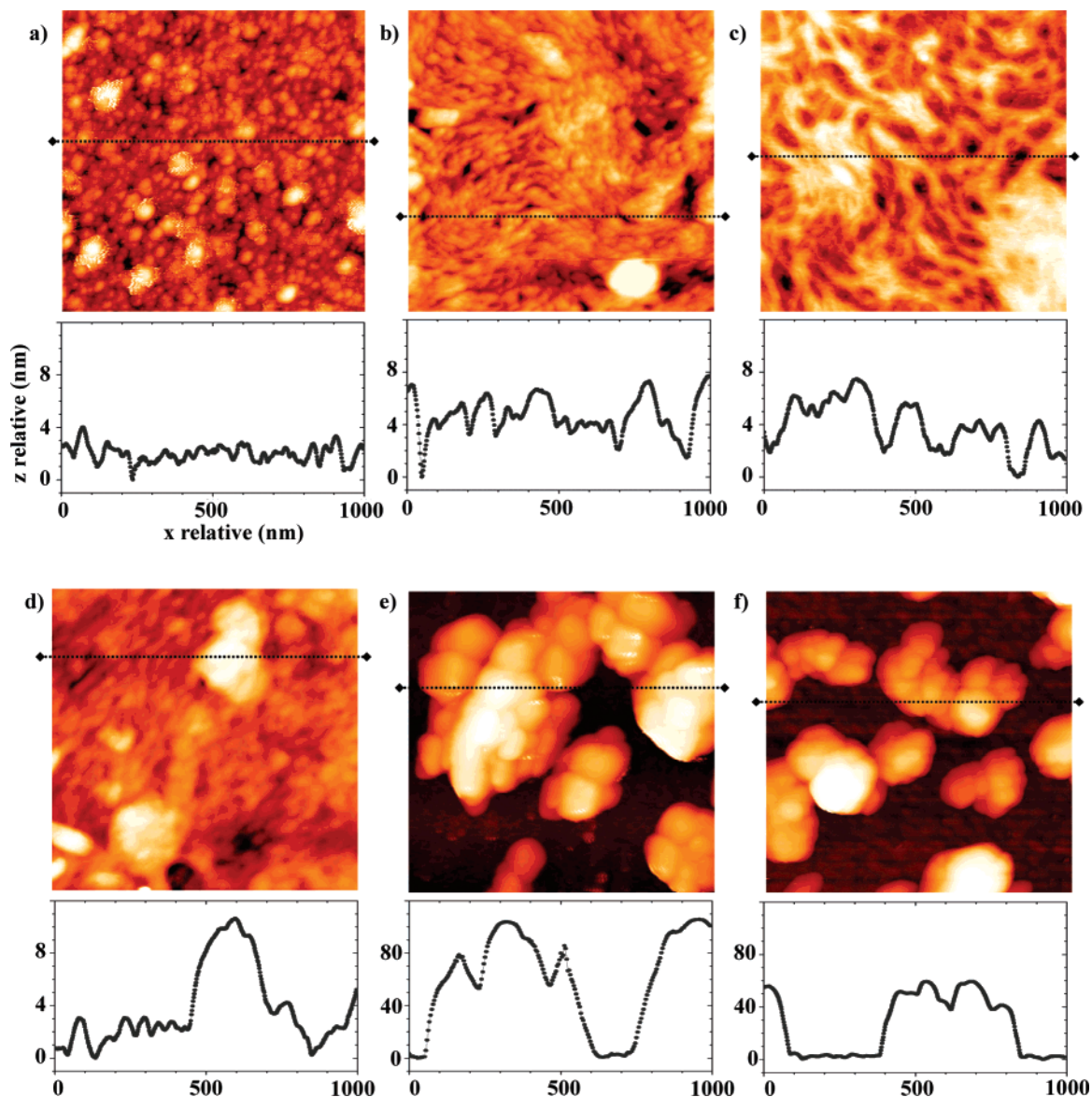
Figure 7. Typical TM-AFM images (1 μm × 1 μm) of both pure and representative hybrid films including their corresponding relative height profiles: (a) bare ITO/glass substrate; (b) CELL-R film; (c) CELL + HOGaPc film; (d) 1-HOGaPc/CELL-R film; (e) 7-HOGaPc film; (f) 7-HOGaPc/CELL-R film.

a sample.[26,33] The presence of adsorbed molecules changes the value of the surface potential due to the addition of their dipole moments to the surface. These measurements enable us to identify and screen rapidly the sorption processes. We have profited from this methodology bearing in mind two aspects. On one hand, it allowed us to analyze the electrical properties of the ITO-covering films. On the other, the changes in this surface property could be also utilized as a principle of transduction in eventual gas-sensing applications (vide infra).[6,33]

Therefore, to show the effect of cellulose in the properties of the films, we have performed several sensor tests using gas samples with dissimilar activity, namely, the electrically inert N_2 and O_3, a well-known electron acceptor gas and strong pollutant in ecosystems, toxic for all living organisms, including humans.[35] We have chosen the KP technique as transducer of the electrical

changes produced in the thin films after being submitted to the above-mentioned gas flows.[33] The changes in ΔU_s respond to modifications of the electrostatic potential of the films due to variations of the overall surface dipole moment. These alterations can be measured as a principle of gas-sensing transduction, for instance in Gate-modified field effect transistors (Gate-FETs),[36] and more recently in the molecular controlled semiconductor resistor (MOCSER), described by Cahen et al.[24] and Rei Vilar et al.[25] According to this concept, 2-D arrangements of molecules can lead to particular cooperative effects able to be applied in gas sensing through electrostatic effects. This proposes an alternative to the transfer of matter and charge between the locus of sensing and that of detection, which is occasionally somewhat inefficient in organic materials, mainly when bulky films are used.

Figure 8 illustrates the ΔU_s changes observed when a 1-HOGaPc/ITO film (a) and a 1-HOGaPc/CELL-R/ITO film are submitted to alternate atmospheres of N_2 and 100 ppb of O_3.

(33) Taylor, D. M.; Morgan, H.; D'Silva, C. *J. Phys. D: Appl. Phys.* **1991**, *24*, 1443.

(34) (a) Oprea, A.; Weimar, U. *Sens. Actuators, B* **2005**, *111−112*, 572. (b) Potje-Kamloth, K. *Crit. Rev. Anal. Chem.* **2002**, *32*, 121.

(35) Kondratyev, K. Y.; Varotsos, C. A. *Environ. Sci. Pollut. Res. Int.* **1996**, *3*, 205.

(36) Barker, P. J.; Petty, M. C.; Monkman, A. P.; McMurdo, J.; Cook, M. J.; Pride, R. *Thin Solid Films* **1996**, *284−285*, 94.
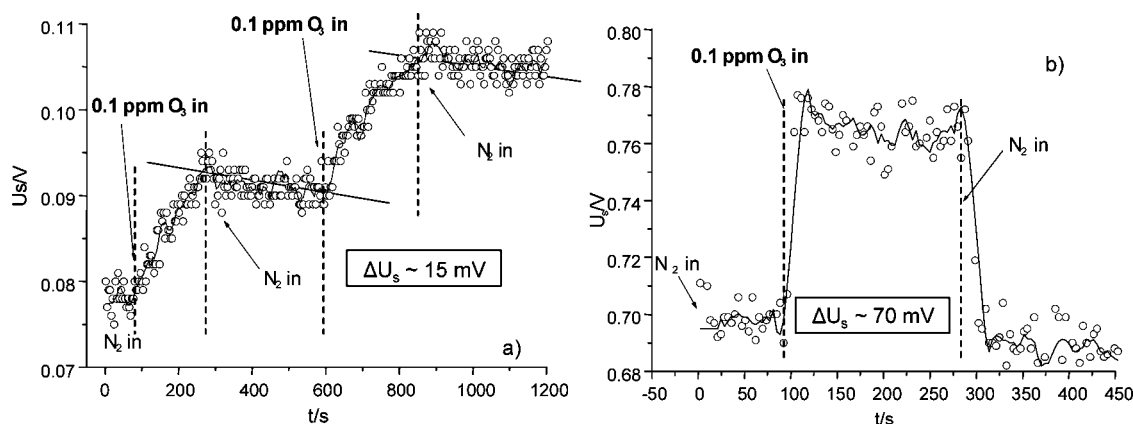
Figure 8. Transient response of the surface potential after the alternate exposure from inert N_2 to an electron-accepting agent as O_3 (100 ppb) measured using the Kelvin probe: (a) in a 1-HOGaPc/ITO film; (b) in a 1-HOGaPc/CELL-R/ITO hybrid film.

It has to be pointed out that these tests have been carried out in a real environment, i.e., at room atmosphere. As HOGaPc can be considered as a p-type molecular semiconductor, it is expected that, after adsorption, the oxidizing O_3 leads to the formation of positively charged phthalocyanines at the surface,[9a] $[HOGaPc]^+$, that should contribute to the modification of the resultant surface dipole due to the surface polarization.[37] In Figure 8a, when N_2 is applied during a period of 100 s, no changes in U_s are detected. On the contrary, a progressive increasing of U_s up to ca. 15 mV is clearly observable after exposing the film to a similar flow of 100 ppb O_3 in air during 200 s. Afterward, if we expose the film again to the N_2 flow, a slow and linear recovering of the initial U_s value is observed. This indicates that the adsorption kinetics are much faster than the desorption process. Nonetheless, this overall behavior is reproducible, as shown by the second cycle of gas exposure.

Markedly different is the trend followed by the hybrid film (Figure 8b) under analogous conditions. Following inert behavior in N_2 atmosphere, the application of the O_3 flow leads to an extremely fast and linear augmentation of U_s (ca. 70 mV after half a minute of exposure). Subsequently, a plateau is attained and upheld after 170 s of additional exposure. At this moment, once the N_2 flow has substituted the oxidizing one, the initial baseline is rapidly restored. This suggests that, in this case, the hybrid film not only acts as an active layer in detecting the oxidant atmosphere with higher sensitivity and stability but also exhibits a fast recovery of the initial properties. The synergetic relation between components leads to enhanced sensing performances. This fact should be related to the adsorption and gas diffusion properties of cellulose film due to its porous-based nature and inner surface. The large plateau observed in U_s value during O_3 exposure supports this statement. Contrarily, the reported reactivity of cellulose vs O_3, usually associated to the depolymerization of chains via transformation of model cellulose compounds, namely, glucose and cellobiose,[38] should be rather discarded following the next criteria: (i) the concentration of O_3 in our experiments is highly diluted in air; (ii) the degradation reactions are reported in aqueous medium and under strong conditions. Recently, it has been proved that ozonation of lignocellulosic fibers improves the bulky properties in terms of absorption processes (wettability) without damaging the surface chemistry.[39] Finally, as seen, the surface potential baseline is easily recovered, supporting the chemical inertia of cellulose in

the transient 100 ppb O_3/air atmosphere. We also discard eventual interactions between O_3 and ITO, typically occurring in samples at high temperatures and in strong ozone-based environments (ozone-plasma).[40]

The intriguing difference observed in the ozone-sensing performances of 1-HOGaPc/ITO and 1-HOGaPc/CELL-R/ITO films may be explained as follows. First, in case of the 1-HOGaPc/ITO system, we can consider a typical combined process consisting of a gas adsorption + charge-transfer phenomenon at the molecular material surface that leads to changes in the surface potential. The variation of U_s should be then ascribed to a surface polarization followed by a charge transfer ($[Ox^+ \cdot Pc^-]$). Both the monotonous U_s increasing and the subsequent slow signal recovering should be explained in terms of a simultaneous surface and bulky effect caused by the island-like structure of the phthalocyanine during the charge-transfer process. Actually, AFM, UV−vis, and XPS analyses have shown that phthalocyanine is much more dispersed and less aggregated when deposed on cellulose than on ITO, for the same number of depositions. This means that the specific surface, the exposed surface of phthalocyanine, is much larger in 1-HOGaPc/CELL-R/ITO than in the 1-HOGaPc/ITO case. This would explain both the larger variation of signal and the faster signal recovering due to the presence of cellulose in the film.

Thus, these two examples illustrate that the sensitivity and variability of responses depending on the film composition suggest encouraging research regarding the potential use of cellulose-based films as active elements for gas sensors. However, many other applications can be projected by using hybrid films based on cellulose and different molecular materials as phthalocyanines. Regarding the present system, we are currently studying the photophysical properties of HOGaPc in different cellulose environments. Besides, the incorporation via chemical linkage of other phthalocyanine and porphyrin derivatives is also underway.

Conclusions

In this work, we have presented a new family of hybrid thin films based on nanometric cellulose (from a trimethylsilyl derivative, after a simple regeneration process) films as a polymer support, using hydroxygallium phthalocyanine (HOGaPc) as functional molecular material, due to its particular properties. The main features of these films are their straightforward preparation method (by spin-coating), control of deposition (as proved by FTIR in ATR/MIR mode, UV−vis, and XPS

(37) Muzikante, I.; Parra, V.; Dobulans, R.; Fonavs, E.; Latvels, J.; Bouvet, M. Submitted for publication in *Org. Electron.*
(38) Lemeune, S.; Barbe, J. M.; Trichet, A.; Guilard, R. *Ozone: Sci. Eng.* **2000**, *22*, 447.
(39) Östenson, M.; Gatenholm, P. *Langmuir* **2005**, *21*, 160.

(40) Gurlo, A.; Bârsan, N.; Ivanovskaya, M.; Weimar, U.; Göpel, W. *Sens. Actuators, B* **1998**, *47*, 92.

spectroscopies), and potential properties, for instance, as sensing elements in gas sensors. The mechanism of HOGaPc interaction with cellulose is essentially physisorption. AFM analysis has demonstrated that the phthalocyanine tends to form islands over cellulose, whose size and structure are controlled by the cellulose support thanks to an attenuated growth mechanism.

Regarding the gas-sensing tests, the hybrid films exhibited much more enhanced sensing performances toward active gases as ozone, even at very low concentrations (100 ppb in air). This effect was attributed to the different arrangement of phthalocyanine on cellulose and on ITO. The phthalocyanine specific surface is much larger when deposited on cellulose than when it is deposited on ITO; the HOGaPc/CELL-R/ITO sample exposes, then, a much larger number of active molecules to the ozone stream.

The synergetic effect induced by cellulose in the structure and properties of the films places this biopolymer as a great candidate for the building of functional hybrid films, due to its processability and physicochemical skills.

We also note the potential use of cellulose as a versatile coverage element for semiconductor surfaces (for instance, unstable, as GaAs) thanks to the formation of functionalized films by its modification via physical and/or chemical approaches.

Supporting Information Available: An UV−vis spectrum of a HOGaPc solution in $CHCl_3$ (Figure S1) and two XPS analyses (Ga 2p region) for 1-HOGaPc/ITO and 1-HOGaPc/CELL-R/ITO spun films (Figure S2), at two different analysis angles, 90 and 30°, relative to the sample surface. This material is available free of charge via the Internet at http://pubs.acs.org.

LA063114I